Electronic Supplementary Information

Surface Engineering of Rh-Modified Pd Nanocrystals by Colloidal Underpotential Deposition for Electrocatalytic Methanol Oxidation

Haibo Bao, Shiyu Xia, Fengxia Wu, Fenghua Li, Ling Zhang, Yali Yuan, Guobao Xu, and Wenxin Niu*

* Corresponding author. E-mail: niuwx@ciac.ac.cn

Contents

Modeling the shell thickness of Rh-modified Pd octahedral nanocrystals

For an octahedral nanocrystal, the total volume V_{total} can be determined by following equation:

$$V_{total} = \frac{\sqrt{2}}{3}a^3 \tag{1}$$

where a is the edge length of octahedral nanocrystal, which can be measured by related TEM images the average edge length a was measured to be 63 ± 4 nm (Fig. S8). Similarly, the total surface area is given by:

$$S = 2\sqrt{3}a^2 \tag{2}$$

The total number of atoms and surface atoms can be determined by:

$$n_{total} = N_A * \frac{\rho V_{total}}{A_r} \tag{3}$$

$$n_{surf} = S * \rho_{(111)} \tag{4}$$

Where $\rho(111)$ is estimated to be 1.6×10^{15} cm^{-2}, which is the average Rh atoms density in the (111) facet, assuming monolayer of Rh was covered on Pd. Since the lattice constants of Pd and Rh are similar, the density of nanocrystal ρ and relative atomic mass A_r is approximately estimated to be that of pure Pd (12.023 g cm^{-3}, 106.42), respectively. The ratio of n_{surf}/n_{total} can be considered equal to the molar concentration of Rh:

$$\frac{n_{surf}}{n_{total}} = x_{Rh} \tag{5}$$

By substituting Eq. (1-4) into Eq. (5), x_{Rh} was calculated to be 0.027 ± 0.002, in general agreement with the experimental value of 0.03 measured by ICP analysis. Thus, it is concluded that Pd octahedral nanocrystal is covered with about monolayer of Rh.

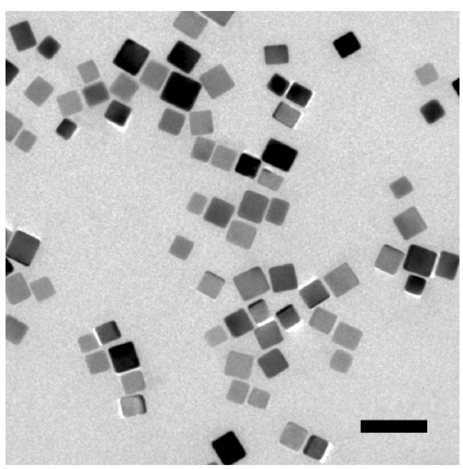

Fig. S1. TEM image of Pd cubic seeds (size: 20±2 nm) for synthesis of Pd-based nanocrystals. Scale bar: 50 nm.

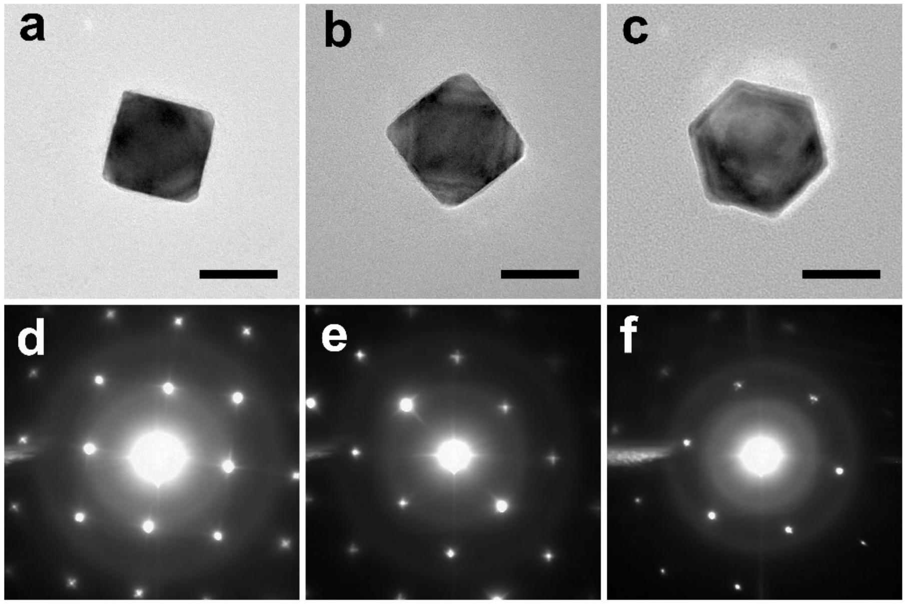

Fig. S2. TEM images and corresponding SAED patterns of a single nanocrystal under different Rh(III)/Pd(II) precursor ratios: (a, d) 0.16, mildly truncated cube (b, e) 0.64, truncated cube (c, f) 1.92, octahedral nanocrystal. Zone axis: [001] for (d,e) and [111] for (f), respectively. Scale bars: 50 nm.

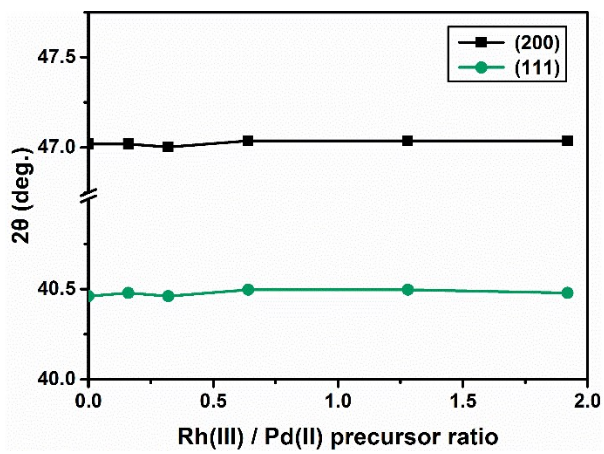

Fig. S3. Detailed (111) and (200) diffraction peak positions of Pd-based nanocrystals with respect to different precursor molar ratios.

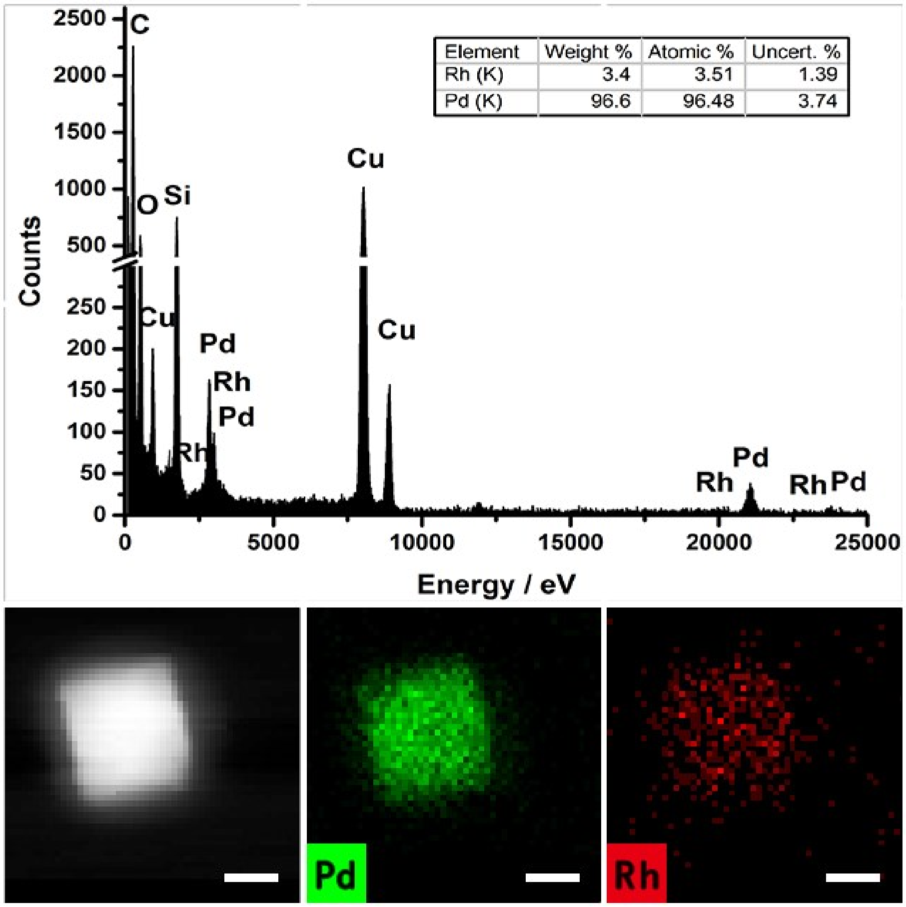

Fig. S4. EDS spectrum and elemental mapping images of Rh-modified Pd octahedral nanocrystals. Scale bars: 30 nm.

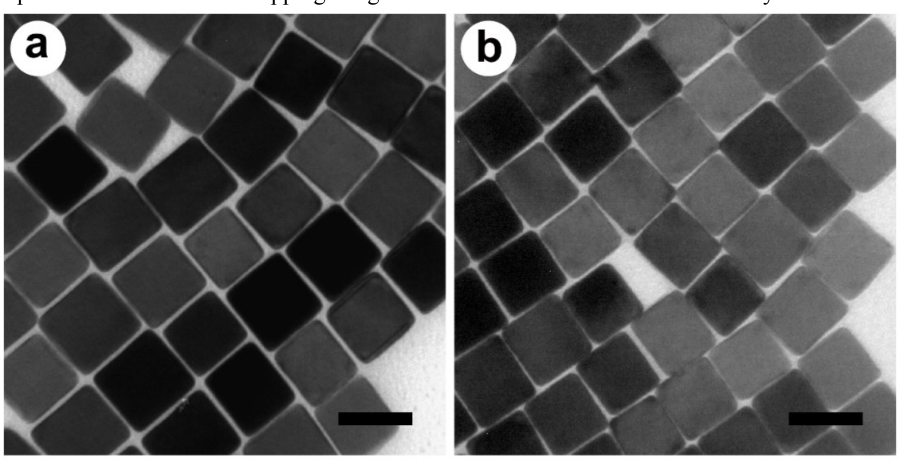

Fig. S5. TEM images of Pd-based nanocrystals before (a) and after (b) growth reaction in the absence of H_2PdCl_4 precursor, other conditions are the same as the growth of Rh-modified Pd-based nanocrystals. Pd nanocubes of 48±3 nm in size were used as seeds. Scale bars: 50 nm.

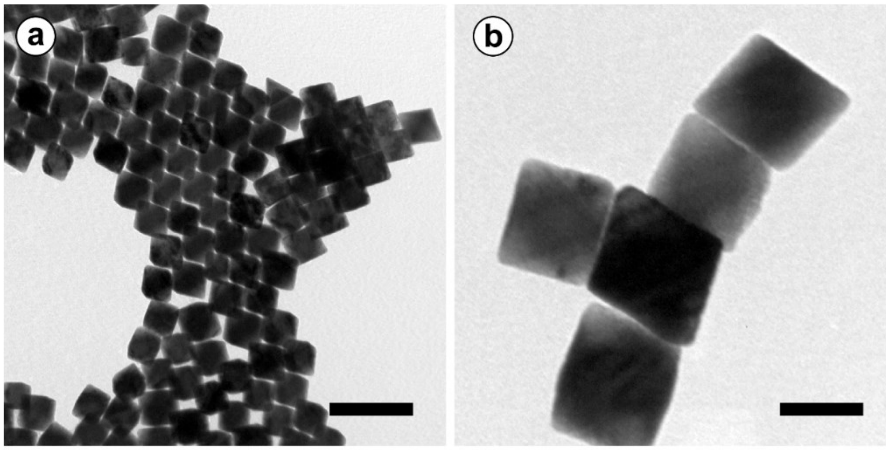

Fig. S6. TEM images of pristine Pd octahedral nanocrystals with exposed {111} facets for electrochemical measurements. Scale bars: (a) 200 nm; (b) 50 nm.

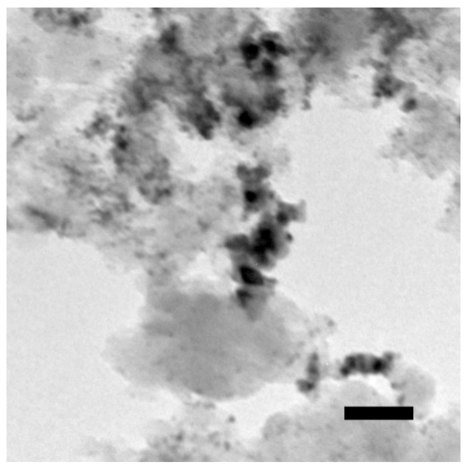

Fig. S7. TEM image of commercial Pd/C (10 wt.%) catalysts. Scale bar: 50 nm.

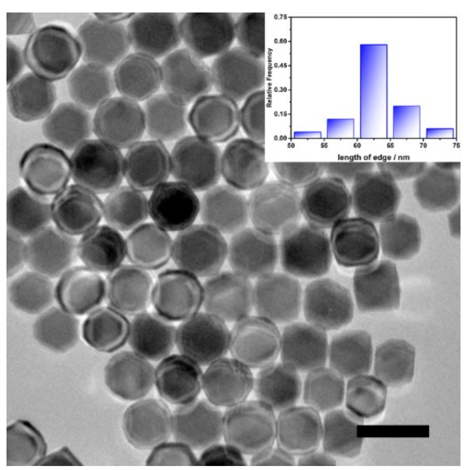

Fig. S8. TEM characterization of Rh-modified nanocrystals; the inset shows the size distribution of Rh-modified Pd octahedral nanocrystals. Scale bar: 100 nm.

Table S1. ICP results of Pd-based nanocrystals synthesized with different ratios of Rh(III)/Pd(II) precursors.

Rh(III)/Pd(II) precursor ratio	Mass percentage of Rh (%)	Molar percentage of Rh (%)	Corresponding morphology
0	0	0	Cube
0.16	2.16	2.24	Slightly truncated cube
0.32	2.21	2.28	Truncated cube
0.64	2.90	3.00	cuboctahedron
1.28	2.96	3.06	Truncated octahedron
1.92	2.93	3.03	Octahedron